A Novel Class of Generalized Chebyshev Low-Pass Prototype for Suspended Substrate Stripline Filters

SAOD A. ALSEYAB

Abstract—**A novel class of low-pass prototype filters having an equiripple passband response with three transmission zeros at infinity and the remainder at a finite real frequency is presented. The prototypes are synthesized using the alternating pole technique to obtain directly the even-mode or the odd-mode admittance and little accuracy is lost for prototypes up to degree 15. Tables of element values for commonly used specifications are included. The tables are useful for the design of TEM-mode microwave broad-band filters, diplexers, and multiplexers, particularly for a printed circuit form a realization. A design example of a low-pass microwave broad-band filter designed and constructed in suspended substrate stripline (SSS) configuration is given and experimental results are also presented.**

I. Introduction

THIS PAPER introduces a very selective class of low-pass prototype networks which have important applications in the design of TEM-mode microwave broad-band filters, diplexers, and multiplexers, particularly for a printed circuit form of realization. This network satisfies a generalized Chebyshev response with an equiripple passband, has three transmission zeros at infinity, and an even multiple of transmission zeros at a finite point on the $j\omega$-axis close to the bandedge. Its selectivity is therefore very close to the same degree optimum as the elliptic function filter but is much easier to realize physically. This is due to the fact that the basic problem with the elliptic function filter is that for normally required specifications, there can exist up to a 10:1 variation in impedance values of elements in the physical structure. This would cause severe problems with the printed circuit realization while the impedance variation in the filters based on the generalized Chebyshev prototypes is typically less than 2:1. Furthermore, this prototype has better selectivity and flexibility to tune than the recently introduced generalized Chebyshev prototype having a single transmission zero at infinity and the remainder at a finite real frequency [1].

In Section II of this paper, a description of the generalized Chebyshev response of the prototype is presented. A numerical example is given to illustrate the synthesis procedure based on the alternating pole technique [1]. In Section III, a design example of a low-pass microwave broad-band filter constructed in a suspended substrate stripline (SSS) structure is presented together with the experimental results. Tables of element values for typical requirements are provided in the Appendix. A design chart is also given to help the designer in estimating the required degree of the filter.

Manuscript received September 24, 1981; revised March 26, 1982.

The author is with the Department of Electrical Engineering, College of Engineering, University of Basrah, Basrah, Iraq.

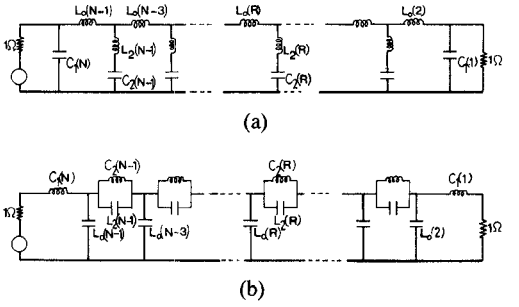

Fig. 1. (a) A generalized Chebyshev low-pass prototype filter having 3 transmission zeros at infinity and $(N-3)$ at a finite frequency. (b) The dual.

II. The Generalized Chebyshev Prototype

The doubly terminated low-pass prototype network shown in Fig. 1 satisfies a generalized Chebyshev insertion-loss (IL) response described by

$$\mathrm{IL} = 1 + \epsilon^2 \cosh^2 \left\{ (N-3) \cosh^{-1} \left[\omega \left(\frac{\omega_0^2 - 1}{\omega_0^2 - \omega^2} \right)^{1/2} \right] + 3 \cosh^{-1} \omega \right\} \quad (1)$$

and can be obtained using the principles presented in [2] and [3]. The transmission zeros are of order $(N-3)$ at $\omega = \pm \omega_0$ and three at finity, N is an odd number equal to the degree of the network,

$$\epsilon = [10^{(\mathrm{RL}/10)} - 1]^{-1/2} \quad (2)$$

and RL is the minimum return loss level (dB) in the passband.

A typical insertion-loss response is illustrated in Fig. 2, where ω_m is the frequency of the minimum insertion-loss level (IL_m) in the stopband and ω_1 is the bandedge frequency of the stopband. ω_m and ω_1 are derived numerically by iteration (e.g., Newton–Raphson technique) for the given values of N, IL_m, and RL.

0018-9480/82/0900-1341$00.75 ©1982 IEEE

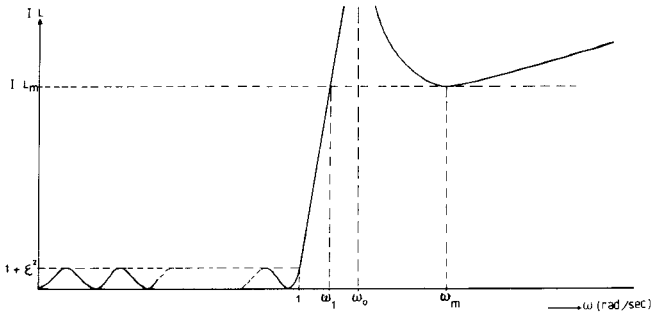

Fig. 2. The generalized Chebyshev insertion-loss response.

If (1) is written in a general form as

$$\mathrm{IL} = 1 + \epsilon^2 F_N^2(\omega) \tag{3}$$

where $F_N(\omega)$ is a general Chebyshev rational function, then ω_m is defined by

$$\left.\frac{dF_N(\omega)}{d\omega}\right|_{\omega=\omega_m} = 0$$

yielding

$$\omega_m^2 = \omega_0^2 + \frac{(N-3)}{3}\omega_0\left(\omega_0^2 - 1\right)^{1/2}. \tag{4}$$

Hence, ω_0 can be determined. One can then proceed to find the element values of the prototype.

However, it has been found that it is not possible to carry out the synthesis of high-degree networks of this type by using the conventional methods (e.g., extracting elements in the p-plane or using the Z-transformed technique) without losing a significant amount of accuracy. Therefore, the alternating pole synthesis technique [1] has been adopted. To find the element values of the network, it is necessary to construct either Y_e or Y_o uniquely from the poles of $S_{11}(p)$, where $Y_e(Y_o)$ is the input admittance when an open (short) circuiting plane is inserted along the line of symmetry of the network. Using the bisection theorem and the principles presented in [1], the transfer and reflection coefficients are expressed in terms of Y_e and Y_o as

$$S_{12}(p) = \frac{Y_e - Y_o}{(1+Y_e)(1+Y_o)} \tag{5}$$

$$S_{11}(p) = \frac{1 - Y_e Y_o}{(1+Y_e)(1+Y_o)} \tag{6}$$

where Y_e and Y_o are reactance functions. But

$$|S_{12}(j\omega)|^2 = \frac{1}{1+\epsilon^2 F_N^2(\omega)} = \frac{1}{[1+j\epsilon F_N(\omega)][1-j\epsilon F_N(\omega)]} \tag{7a}$$

and

$$|S_{11}(j\omega)|^2 = 1 - |S_{12}(j\omega)|^2 = \epsilon^2 F_N^2(\omega)/[1+\epsilon^2 F_N(\omega)] \tag{7b}$$

$$\therefore j\epsilon F_N(\omega) = \frac{S_{11}(j\omega)}{S_{12}(j\omega)} = \pm\left(\frac{Y_e Y_o - 1}{Y_e - Y_o}\right). \tag{8}$$

Hence

$$\frac{1}{1 - j\epsilon F_N(p/j)} = \frac{Y_o - Y_e}{(Y_e+1)(Y_o-1)} \tag{9}$$

and

$$\frac{1}{1 + j\epsilon F_N(p/j)} = \frac{Y_e - Y_o}{(Y_o+1)(Y_e-1)}. \tag{10}$$

Since Y_e and Y_o are reactance functions, it appears from (9) that the left-half zeros of $(1 - j\epsilon F_N(p/j))$ are zeroes of (Y_e+1). Similarly, from (10), the left-half Zero of $(1 - j\epsilon F_N(p/j))$ are zeros of (Y_o+1).

However, a Hurwitz polynomial can be constructed either from the left-half zeros of $(1 - j\epsilon F_N(p/j))$ to form Y_e or from the left-half zeros of $(1 + j\epsilon F_N(p/j))$ to form Y_o. These two sets of left-half zeros are the poles of $S_{11}(p)$. By obtaining the poles of $S_{11}(p)$ numerically, either set can be identified by taking poles in alternating order from the largest imaginary part.

The synthesis procedure can be illustrated by the following numerical example.

Given: The degree $N = 9$, $\mathrm{IL}_m = 60$ dB, $\epsilon = 0.1$, RL = 20 dB, it is required to find the element values of the network shown in Fig. 3.

The numerical solution gives $\omega_0 = 1.32599$ rad/s and the poles of $S_{11}(p)$ are

$$\begin{aligned} p_{1,9} &= -0.030333 \pm j1.02275 \\ p_{2,8} &= -0.10604 \pm j0.96344 \\ p_{3,7} &= -0.225112 \pm j0.80937 \\ p_{4,6} &= -0.377114 \pm j0.490176 \\ p_5 &= -0.455417. \end{aligned}$$

The network can be synthesized by constructing Y_e, which is obtained by forming a Hurwitz polynomial such as

$$\begin{aligned} D(p) &= [p + 0.030333 - j1.02275] \\ &\quad \cdot [p + 0.030333 + j1.02275] \\ &\quad \cdot [p + 0.225112 - j0.80937][p + 0.225112 + j0.80937] \\ &\quad \cdot [p + 0.455417] \\ &= 0.455417 + 1.31691p + 1.793p^2 + 2.72394p^3 \\ &\quad + 1.30779p^4 + 1.3533p^5. \end{aligned}$$

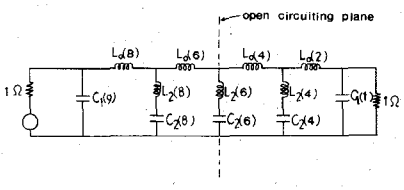

Fig. 3. A network of degree 9.

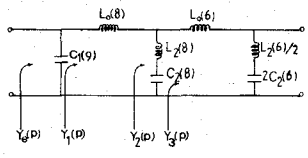

Fig. 4. The synthesis cycle.

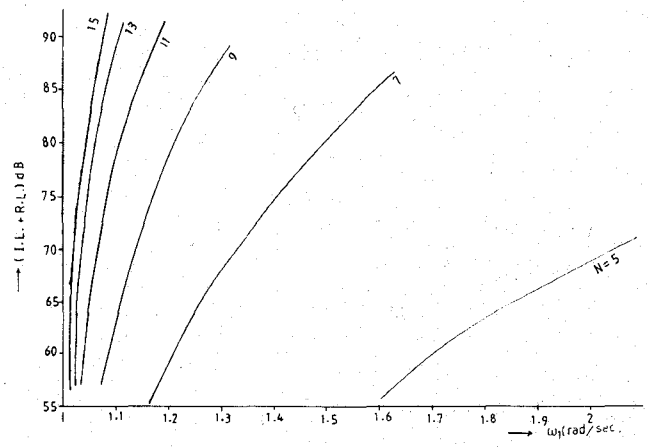

Fig. 5. The design chart for the generalized Chebyshev filter.

Rearranging the odd and even terms in P results in $D(p) = O(p) + E(p)$ where

$$O(p) = 1.31691p + 2.72394p^3 + 1.3533p^5 = A(1)p + A(3)p^3 + A(5)p^5$$

and

$$(p) = 0.455417 + 1.793p^2 + 1.30779p^4 = B(0) + B(2)p^2 + B(4)p^4.$$

Hence

$$Y_e(p) = \frac{O(p)}{E(p)}.$$

The synthesis procedure commences with the extraction of the shunt capacitor $C_1(9)$ by completely removing a pole at infinity from $Y_e(p)$ to leave

$$Y_1(p) = Y_e(p) - C_1(9)p$$

where

$$C_1(9) = \left.\frac{Y_e(p)}{p}\right|_{p=\infty} = \frac{A(5)}{B(4)} = 1.03487.$$

Hence

$$Y_1(p) = \frac{A_1(1)p + A_1(3)p^3}{B(0) + B(2)p^2 + B(4)p^4}$$

$$A_1(1) = A(1) - C_1(9)B(0) = 0.845557$$

$$A_1(3) = A(3) - C_1(9)B(2) = 0.868418$$

$$Z_1(p) = \frac{1}{Y_1(p)}.$$

The series inductance $L_0(8)$ is extracted by a zero-shifting step such that

$$L_0(8) = \frac{Z_1(j\omega_0)}{j\omega_0} = \frac{1}{j\omega_0}\,\frac{B(0) - B(2)\omega_0^2 + B(4)\omega_0^4}{jA_1(1)\omega_0 - jA_1(3)\omega_0^3} = 1.12352$$

$$Z_2(p) = Z_1(p) - L_0(8)p = \frac{B_1(0) + B_1(2)p^2 + B_1(4)p^4}{A_1(1)p + A_1(3)p^3}$$

where

$$B_1(0) = B(0)$$

$$B_1(2) = B(2) - A_1(1)L_0(8) = 0.842999$$

$$B_1(4) = B(4) - A_1(3)L_0(8) = 0.332105$$

$$Y_2(p) = \frac{1}{Z_2(p)}$$

$$Y_3(p) = \frac{p/L_2(8)}{p^2 + \omega_0^2}.$$

$L_2(8)$ can be calculated by finding the residue K_8 at $\pm j\omega_0$ of $Y_2(p)$. Thus

$$K_8 = \left.\frac{A_1(1)p + A_1(3)p^3}{\frac{d}{dp}\{B_1(0) + B_1(2)p^2 + B_1(4)p^4\}^2}\right|_{p=\pm j\omega_0} = 1.04847$$

$$L_2(8) = 1/(2K8) = 0.476885$$

$$C_2(8) = 1/(L_2(8)\omega_0^2) = 1.19263$$

and the cycle is repeated to obtain the remaining element values of half the symmetrical network shown in Fig. 4. The complete element values of this example are included in Table III.

A. Results

For the prototype network shown in Fig. 1, all the element values provided in Tables (I–VI) in the Appendix have been obtained by using the alternating pole technique to construct either Y_e or Y_o, whichever has the highest degree. It has been found that networks of degree 5, 9, and 13 can be synthesized by constructing Y_e, while networks of degree 7, 11, and 15 can be synthesized by constructing Y_o. However, in either case, the element values may be obtained by using a similar procedure to that used in the previous example. Table VII contains the values of ω_0 and ω_1 for the different specifications and the corresponding element values are given in Tables I–VI.

Also, a design chart is given in Fig. 5 showing the

TABLE I

N=5		R.L. ≥ 20 dB			R.L. ≥ 26 dB		
R	Element	I.L.≥60 (dB)	I.L.≥50 (dB)	I.L.≥40 (dB)	I.L.≥60 (dB)	I.L.≥50 (dB)	I.L.≥40 (dB)
5	$C_1(5)$	0.97692	0.980116	0.985092	0.771053	0.773927	0.778435
4	$L_0(4)$	1.30282	1.26448	1.2068	1.25245	1.22001	1.17048
	$L_2(4)$	8.54378×10^{-2}	0.138258	0.227543	7.36741×10^{-2}	0.119383	0.196755
	$C_2(5)$	1.62304	1.5241	1.37499	1.4518	1.37501	1.25759
2	$L_0(2)$	1.30282	1.26448	1.2068	1.25245	1.22001	1.17048
1	$C_1(1)$	0.97692	0.980116	0.985022	0.771053	0.773927	0.778435

TABLE II

N=7		R.L.≥20(dB)			R.L. ≥26(dB)		
R	Element	I.L.≥60 (dB)	I.L.≥50 (dB)	I.L.≥40 (dB)	I.L.≥60 (dB)	I.L ≥50 (dB)	I.L.≥40 (dB)
7	$C_1(7)$	1.01858	1.02211	1.02647	0.816773	0.820282	0 824706
6	$L_0(6)$	1.2363	1.16791	1 08027	1.21518	1.15125	1.06753
	$L_2(6)$	0.256163	0.3682	0 541922	0.233173	0.335228	0.492702
	$C_2(6)$	1.45916	1.29965	1.10006	1.36698	1.23372	1.06387
4	$L_0(4)$	1.2498	1.1300	0.984147	1.30698	1.19918	1 06617
	$L_2(4)$	0.256163	0.3682	0.541922	0.233173	0.335228	0 492702
	$C_2(4)$	1 45916	1.29965	1.10006	1.36698	1.23372	1.06387
2	$L_0(2)$	1.2363	1.16791	1.08027	1.21518	1 15125	1.06753
1	$C_1(1)$	1.01858	1.02211	1.02647	0.816773	0.820282	0.824706

TABLE III

N = 9		R.L. ≥20 (dB)			R.L.≥ 26 (dB)		
R	Element	I.L.≥60	I.L.≥50	I.L.≥40	I.L.≥60	I.L.≥50	I.L.≥40
9	$C_1(9)$	1.03487	1.03721	1.03969	0.83549	0.837985	0.840714
8	$L_0(8)$	1.12352	1.04292	0.947416	1.10722	1.0264	0.928279
	$L_2(8)$	0.476885	0.654003	0.930679	0.450961	0.618263	0.877829
	$C_2(8)$	1.19263	1.01488	0.813568	1.13819	0.980696	0.799104
6	$L_0(6)$	1.07413	0.944115	0.8009	1.15782	1.03493	0.898068
	$L_2(6)$	0.428164	0.569346	0.771466	0.394432	0.521907	0.70086
	$C_2(6)$	1.32834	1.16578	0.98147	1.30131	1.16176	1.00088
4	$L_0(4)$	1.07413	0.944115	0 8009	1.15782	1.03493	0.898068
	$L_2(4)$	0.476885	0.654003	0.930679	0.450961	0.618263	0.877829
	$C_2(4)$	1.19263	1.01488	0.813568	1.13819	0.980696	0.799104
2	$L_0(2)$	1.12352	1.04292	0.947416	1.10722	1.0264	0.928279
1	$C_1(1)$	1.03487	1.03721	1.03969	0.83549	0.837985	0.840714

TABLE IV

N = 11		R L ≥ 20 (dB)			R L ≥ 26 (dB)		
R	Element	I.L.≥60 (dB)	I.L.≥50 (dB)	I.L.≥40 (dB)	I.L.≥60 (dB)	I L.≥50 (dB)	I.L.≥40 (dB)
11	$C_1(11)$	1.0416	1.04297	1.04428	0.843579	0.845115	0.846644
10	$L_0(10)$	1.01792	0.935065	0.840267	0.994819	0 907422	0.804735
	$L_2(10)$	0.729441	0.984313	1.39582	0.710293	0.959304	1.36035
	$C_2(10)$	0.958626	0.787121	0.60441	0.918352	0.760814	0.590439
8	$L_0(8)$	0.908631	0.786767	0.661279	0.995387	0.877259	0.755266
	$L_2(8)$	0.61751	0.794605	1.04755	0.576811	0.736593	0.959128
	$C_2(8)$	1.13239	0.975041	0.80535	1.13087	0.990848	0.837434
6	$L_0(6)$	0.93471	0.807267	0.672323	1.03347	0.908381	0.77411
	$L_2(6)$	0.61751	0.794605	1.04755	0.576811	0.736593	0.959128
	$C_2(6)$	1.13239	0.975041	0 80535	1.13087	0.990848	0.837434
4	$L_0(4)$	0.908631	0.786767	0.661279	0.995387	0.877259	0.755266
	$L_2(4)$	0.729441	0.984313	1.39582	0.710293	0.959304	1.36035
	$C_2(4)$	0.958626	0.787121	0.60441	0.918352	0.760814	0.590439
2	$L_0(2)$	1.01792	0.935065	0.840267	0.994819	0.907422	0.804735
1	$C_1(1)$	1.0416	1.04297	1.04428	0.843579	0.845115	0.846644

TABLE V

N = 13		R.L. ≥ 20(dB)		R.L.≥ 26 (dB)	
R	Element	I.L≥ 60 (dB)	I.L ≥50 (dB)	I.L. ≥60 (dB)	I.L. ≥50 (dB)
13	$C_1(13)$	1.04459	1.04538	0 84729	0.848212
12	$L_0(12)$	0.928797	0.847254	0.894132	0.804545
	$L_2(12)$	1.01275	1 36487	1.01212	1.36929
	$C_2(12)$	0.773517	0.616731	0.736698	0.589614
10	$L_0(10)$	0.778798	0.670841	0 862227	0.756986
	$L_2(10)$	0.810049	1 02504	0.764112	0.958028
	$C_2(10)$	0.96708	0.821198	0.975811	0 842726
8	$L_0(8)$	0.80446	0.687232	0.900696	0.783025
	$L_2(8)$	0.795651	1.00249	0.746468	0.931278
	$C_2(8)$	0.98458	0.839663	0.998876	0.866932
6	$L_0(6)$	0.804469	0.687232	0.900696	0.783025
	$L_2(6)$	0.810049	1.02504	0.764112	0.958028
	$C_2(6)$	0.96708	0.831198	0.975811	0.842726
4	$L_0(4)$	0.778798	0.670841	0.862227	0.756986
	$L_2(4)$	1.01275	1 36487	1.01212	1.36929
	$C_2(4)$	0.773517	0.616731	0.736698	0.589614
2	$L_0(2)$	0.928797	0.847254	0.894132	0.804545
1	$C_1(1)$	1.04459	1.04538	0.84729	0.848212

TABLE VI

N = 15		R.L.≥20 (dB)	R.L.≥26 (dB)
R	Element	I.L.≥60 dB	I.L.≥60 dB
15	$C_1(15)$	1.04601	0.849109
14	$L_0(14)$	0.85466	0.806586
	$L_2(14)$	1.33100	1.36481
	$C_2(14)$	0.629993	0.59235
12	$L_0(12)$	0.680414	0.759946
	$L_2(12)$	1.00399	0.953938
	$C_2(12)$	0.835194	0.847481
10	$L_0(10)$	0.699487	0.788953
	$L_2(10)$	0.977594	0.921391
	$C_2(10)$	0.857741	0.877417
8	$L_0(8)$	0.704337	0.79654
	$L_2(8)$	0.977594	0.921391
	$C_2(8)$	0.857741	0.877417
6	$L_0(6)$	0.699487	0.788953
	$L_2(6)$	1.00399	0.953938
	$C_2(6)$	0.835194	0.847481
4	$L_0(4)$	0.680414	0.759946
	$L_2(4)$	1.331	1.36481
	$C_2(4)$	0.629993	0.59235
2	$L_0(2)$	0.85466	0.806586
1	$C_1(1)$	1.04601	0.849109

TABLE VII

		R.L.≥ 20(dB)			R.L.≥ 26(dB)		
Degree	Frequency	I.L.≥60 (dB)	I.L.≥50 (dB)	I.L.≥40 (dB)	I.L.≥60 (dB)	I.L.≥50 (dB)	I.L.≥40 (dB)
5	ω_0	2.68541	2.17845	1.7878	3.05766	2.46817	2.01033
	ω_1	2.52739	2.04812	1.69345	2.88554	2.3175	1.90012
7	ω_0	1.63565	1.44559	1.29516	1.77125	1.55497	1.38122
	ω_1	1.4999	1.33773	1.21229	1.61703	1.43071	1.28362
9	ω_0	1.32599	1.22745	1.14922	1.3958	1.28424	1.19397
	ω_1	1.21737	1.14178	1.0848	1.27249	1.18496	1.11696
11	ω_0	1.19586	1.13609	1.08873	1.23816	1.17053	1.1158
	ω_1	1.1087	1.06853	1.03927	1.13856	1.09134	1.05564
13	ω_0	1.12983	1.08995		1.15808	1.11293	
	ω_1	1.05953	1.03646		1.07704	1.04948	
15	ω_0	1.09205			1.11218		
	ω_1	1.03489			1.04574		

relationship between ω_1 and (IL+RL) (dB) for different values of N.

III. Design and Performance of a Practical Model

In several applications, especially for satellite and airborne communication and ECM systems, there are continuous demands for smaller size, lighter weight devices, and cheaper manufacturing cost. Filter designs are no exception from this trend. In the past few years, several types of filters have been constructed in stripline or microstrip. They were limited to relatively wide-band applications where the selectivity is not severe. Microstrip and stripline filters suffer from limitations on stopband loss due to quasi-surface modes, higher in-band dissipation loss, and limited range of achievable impedances which limits filter realization, performance, and design flexibility. Furthermore, for highly selective applications, these structures exhibit temperature instability and tuning difficulties. Most recently, two important contributions have been reported [4], [5]. In both of these papers, experimental results on a number of devices constructed in SSS have been given. Those results shows that the SSS is capable of achieving very good electrical performance and temperature stability, and fine tuning is possible with screws in the main enclosure.

This section presents a design example of a 4-GHz cutoff low-pass filter based on the generalized Chebyshev prototype of degree $N=11$, having a minimum stopband insertion loss of 40 dB and minimum passband return loss of 26 dB. The prototype element values are included in Table IV and the corresponding value of $\omega_0 = 1.1158$ rad/s is given in Table VII.

In this design, a 1/2 oz, 0.005-in thick glass reinforced teflon (known commercially as RT/duroid) has been used due to its high level of tolerance on dielectric constant and the thickness of copper and dielectric. The circuit elements are etched on one side of the substrate. The printed board is placed in the middle of a metal box of ground plane spacing b, suitably chosen to prevent the propagation of higher order modes. In this design, $b = 0.07$ in, which also ensures that b is much greater than the dielectric thickness. With this choice the conductors are practically in air, hence the variation of the overall dielectric constant with temperature will be very close to that of air.

However, to transform the lumped prototype element values to the distributed domain, Richard's transformation should be applied

$$p \rightarrow Bt = B\tanh(ap) \tag{11}$$

where the constants a and B can be chosen such that the shunt resonant branches may be realized directly by uniform admittance shunt O/C stubs. Each stub is one quarter of a wavelength long at the finite transmission zero f_0 (GHz).

Consider a typical lumped shunt resonant branch and its proposed microwave printed circuit realization by a uniform admittance O/C stub shown in Fig. 6(a) and (b), respectively. The lumped admittance may be written as

$$Y_2(R) = \frac{C_2(R)p}{1+p^2/\omega_0^2} \tag{12}$$

where $\omega_0^2 = 1/(L_2(R)\cdot C_2(R))$. After applying Richards' transformation, it becomes

$$Y_2(R) = \frac{C_2(R)Bt}{1+B^2t^2/\omega_0^2}. \tag{13}$$

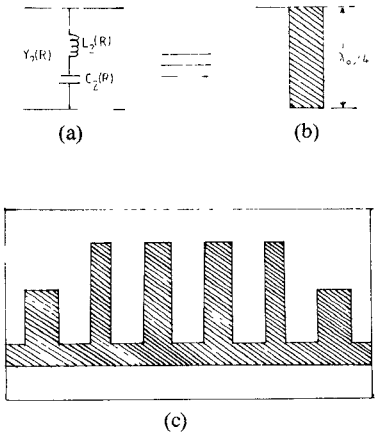

Fig. 6. (a) Lumped shunt resonant section. (b) Shunt O/C resonator stub. (c) Schematic representation of the printed circuit board.

If

$$B = \omega_0 \tag{14}$$

then

$$Y_2(R) = \frac{BC_2(R)t}{1+t^2} \tag{15}$$

$$= \frac{1}{2}BC_2(R)\tanh(2ap) \tag{16}$$

which clearly shows that the shunt resonant branch is realizable by a uniform admittance shunt O/C stub of characteristic admittance

$$Y_{02}(R) = BC_2(R). \tag{17}$$

The constant (a) can be obtained by applying Richards' transformation at the bandedge

$$\omega_c = B\tan(af_c)$$

$$\therefore a = \frac{\omega_c}{f_c}\tan^{-1}(1/B) = 10.466817$$

where $\omega_c = 1$ rad/s, $f_c = 4$ GHz (given), and $B = \omega_0 = 1.1158$. Since the O/C resonant stubs should be quarter-wavelength long at f_0, then, from (16)

$$2af_0 = 90° \qquad f_0 = 4.2993 \text{ GHz}$$

therefore, the length of the resonator is

$$l_r = \frac{\lambda_0}{4} = \frac{v}{4f_0} = 0.686 \text{ in}$$

where v is the velocity of wave propagation.

However, as a direct result of Richards' transformation, the two shunt capacitors $C_1(11)$ and $C_1(1)$ of the lumped prototype network contributing two of the three transmission zeros at infinity are realized by shunt O/C stubs of characteristic admittance

$$Y_{01}(11) = Y_{01}(1) = BC_1(11) = BC_1(1) \tag{18}$$

and they can be made a quarter-wavelength long at $2f_0$. Hence, the length of the O/C stub is

$$l_0 = \frac{\lambda_0}{8} = 0.343 \text{ in.}$$

It remains to realize the series elements $L_0(R)$. These elements are responsible for the third transmission zero at infinity. Due to Richards' transformation, these elements correspond to S/C stubs that produce an infinite impedance when a quarter of a wavelength long at $2f_0$. At this frequency, the two shunt O/C stubs are also a quarter of a wavelength long, each producing an infinite admittance while the shunt O/C resonator stubs are one half of a wavelength long and hence do not contribute to the response of the filter.

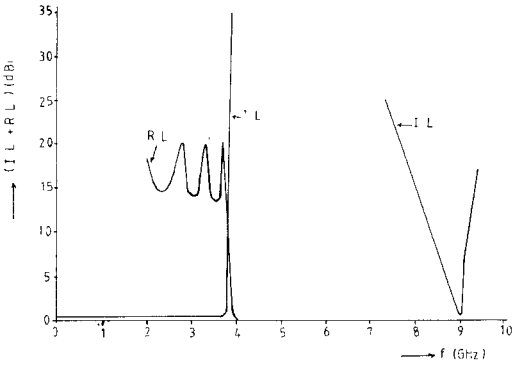

Fig 7. The experimental insertion-loss and return-loss characteristic of the low-pass printed circuit microwave filter.

Since a direct realization of a series S/C stub in printed circuit form is difficult, an alternative is used. It utilizes a length of short transmission line to provide a series-lumped inductive effect on the printed circuit which approximates this type of stub at a frequency below its quarter-wavelength frequency.

Let the lengths of short transmission lines which realize the series-lumped inductances $L_0(R)$ equal $l_s(R) < \lambda_0/8$, and have effective inductances $L_0'(R)$. The actual design values of $L_0'(R)$ can be obtained directly by simple impedance and frequency scaling. Hence

$$L_0'(R) = \frac{R_0 L_0(R)}{2\pi f_c} \tag{19}$$

where R_0 is the actual terminating resistive load. However, the lumped inductance of a short length of line $l_s(R)$ can be approximately given by [6]

$$L_0'(R) = \frac{Z_0 l_s(R)}{V} \tag{20}$$

where Z_0 is the characteristic impedance of the line. Then, from (19) and (20)

$$l_s(R) = \frac{VL_0(R)}{Z_0'} \tag{21}$$

where $Z_0' = Z_0/R_0$ is the normalized characteristic impedance.

The width of the O/C stubs and the short connecting lines are determined from Getsinger's Charts [7]. The printed circuit board is shown schematically in Fig. 6(c).

The low-pass microwave filter has been constructed and tested using a swept frequency reflectometer arrangement. Its experimental insertion-loss and return loss characteristics are obtained as shown in Fig. 7.

IV. Conclusion

A novel class of low-pass prototype filters satisfying a generalized Chebyshev response with three transmission zeros at infinity and the remainder at a finite real frequency has been presented. The prototype has been synthesized using the alternating pole technique. This has been adopted because of its simplicity, while very little accuracy is lost during the synthesis of high-degree networks up to and including degree 15. Tables of the element values for commonly used specifications have been included. The new prototype has the advantage of uniform impedances especially when compared to elliptic function filters. A design example of a low-pass broad-band microwave filter was given. This filter has been designed and constructed in SSS configuration where all of the shunt resonant stubs are of similar impedance. It was necessary to realize the series inductor as short transmission lines. This approximate realization is justified by maintaining the stopband up to an octave above the cutoff frequency as can be seen in Fig. 7. The filters are readily tunable, and are suitable for multiplexer applications.

Appendix

Tables I–VI contain the element values for different degrees of the low-pass prototype filter shown in Fig. 1.

N is the degree of the network.
R is the section.
RL is the return loss in the passband.
IL is the insertion loss in the stopband.
The passband of the network is for $|\omega| \leqslant 1$.
The stopband of the network is from $\omega = \omega_1$ to $\omega = \infty$.
ω_0 is the location of the finite transmission zero on the $j\omega$-axis of the complex frequency plane.

Table VII contains the values of ω_0 and ω_1 for the different specifications.

References

[1] J. D. Rhodes and S. A. Alseyab, "The generalized chebyshev low-pass prototype filter," *Int. J. Circuit Theory and Applications*, vol. 8, pp. 113–125, 1980.
[2] J. Vlach, *Computerized Approximation and Synthesis of Linear Networks*. New York: Wiley, 1969, ch. 8.
[3] J. D. Rhodes, *Theory of Electrical Filters*. New York: Wiley, 1976, pp. 212–214.
[4] J. P. Rooney and L. M. Underkofler, "Printed circuit integration of MW filters," *Microwave J.*, vol. 21, no. 9, pp. 68–73, Sept. 1978.
[5] J. D. Rhodes and J. E. Dean "MIC broad-band filters and multiplexers," in *Proc. 9th Euro. Microwave Conf.*, Sept. 1979.
[6] G. L. Matthaei *et al.*, *Microwave Filters, Impedance Matching Networks and Coupling Structure*. New York: McGraw-Hill, 1964.
[7] W. J. Getsinger, "Coupled rectangular bars between parallel plates," *IRE Trans. Microwave Theory Tech.*, vol. MTT-10, pp. 65–72, Jan. 1962.

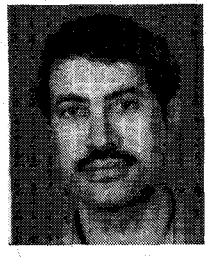

Saod A. Alseyab was born in Abilkhaseeb, southern Iraq, on August 13, 1948. He received the B.Sc. degree in electrical engineering with the equivalent of first-class honors from the University of Basrah, Iraq, in 1969, the M.Sc. and Ph.D. degrees in microwave communications engineering from the University of Leeds, Yorkshire, England, in 1976 and 1979, respectively.

From 1969 to 1974 he was an Instructor and Assistant Lecturer in the Department of Electrical Engineering at the University of Basrah. Presently, he is the Head of the Department of Electrical Engineering, University of Basrah.

Dr. Alseyab's research is on designing microwave filters, diplexers, and multiplexers. He is presently engaged in research on digital filters and analog integrated circuits.